

Transport of Polymer-Coated Metal-Organic Framework Nanoparticles in Porous Media

Satish K. Nune (✉ satish.nune@pnnl.gov)

Pacific Northwest National Laboratory

Quin R.S. Miller

Pacific Northwest National Laboratory

H. Todd Schaeff

Pacific Northwest National Laboratory

Tengyue Jian

Pacific Northwest National Laboratory

Miao Song

Pacific Northwest National Laboratory

Dongsheng Li

Pacific Northwest National Laboratory

B. Peter McGrail

Pacific Northwest National Laboratory

Research Article

Keywords: fate and transport, nanoparticle, polymer, subsurface, heterostructures, nanofluid

Posted Date: November 19th, 2021

DOI: <https://doi.org/10.21203/rs.3.rs-1062071/v1>

License:  This work is licensed under a Creative Commons Attribution 4.0 International License.

[Read Full License](#)

Abstract

Injecting fluids into deep underground geologic structures is a critical component to development of long-term strategies for managing greenhouse gas emissions and facilitating energy extraction operations. Recently, we reported that metal-organic frameworks are low-frequency absorptive acoustic metamaterial that may be injected into the subsurface enhancing geophysical monitoring tools used to track fluids and map complex structures. A key requirement for this nanotechnology deployment is transportability through porous geologic media without being retained by mineral-fluid interfaces. Flow-through column studies were used to estimate transport and retention properties of five different polymer-coated MIL-101(Cr) nanoparticles in siliceous porous media. Nanoparticle transport experiments revealed that nanoparticle surface characteristics play a critical role in nanoparticle colloidal stability and as well the transport.

Introduction

Nanoscale materials in the form of colloidal nanoparticles (nanofluids) are receiving increased attention for industrial and subsurface applications, including geologic carbon storage monitoring,¹ critical material extraction,² enhanced heat transport,³ and hydrocarbon recovery.⁴ At the same time, there is increased recognition of key roles that natural and anthropogenic nanomaterials play in Earth systems, although significant knowledge gaps with regards to nanoparticle fate and transport remain.⁵ Unique properties such as extremely-high surface area, diverse structures, transportability, and tunable surface functionalization make nanoparticles an attractive candidate for subsurface applications, and these properties are exemplified by metal-organic framework (MOF) materials. The metal nodes clusters of these engineered porous materials are connected to organic linkers to produce hierarchically diverse topologies with a plethora of applications, including gas storage, separations, and catalysis.⁶ Considerable attention has been devoted to developing synthesis methods for nanosized MOFs because of their promise in enhanced catalytic, sensing, and adsorption properties relative to bulk MOF forms.^{7,8}

We recently demonstrated that MOFs are low-frequency absorptive acoustic metamaterials, exhibiting anomalous sound transmission loss and tunable resonances from 100-1250 Hz.⁹ These emergent low-frequency properties make MOFs desirable for sound-attenuating applications, including for use as geophysical contrast agent. We have also demonstrated that rocks saturated with MIL-101(Cr)¹⁰ nanofluids (~0.5 wt%) have distinct elastic and anelastic properties, resulting in decreased seismic wave velocities and amplitudes.¹¹ These attributes make injectable MOF nanoparticles a potentially disruptive technology for enabling geologic carbon storage and other subsurface energy storage/extraction endeavors. Our ongoing research involves using injectable colloidal MOF nanoparticles as geophysical contrast agents to help track fluids and delineate structures in the subsurface.

The goal of this present study is to examine how polymer coatings influence the ability of MOF nanoparticles to successfully traverse porous media relevant to geologic carbon storage reservoirs, a

concept illustrated in Figure 1. A key requirement for a MOF nanofluid contrast agent is the ability of particles to be transported in porous geologic media without being immobilized in pores or agglomerated to other nanoparticles. To that end, we studied the effects of different polymer coatings on MOF nanoparticle transport and retention in siliceous porous geologic media, which has not been previously evaluated. Polymer-coated MOF nanoparticle heterostructures were the focus of this work as we have recently demonstrated polymer coatings enhance colloidal stabilities of MOF nanoparticles, even when they are mixed with saline geothermal brines.¹²

Experimental

Materials:

Accusand (Unimin Corporation), whose physical and chemical properties have been described by Schroth et al.¹³, was chosen for unconsolidated sand column experiments. Accusand was utilized as porous media in this study due to its relevant silica-rich composition, defined particle characteristics and common use in nanoparticle transport studies.^{14,15} The grain sizes of the Accusand was sieved to select the 210-841 μm size fraction (mesh 70-20), with 35% of the sand mass found in the 210-420 μm (mesh 20-40) range, and 65% of the mass occupying the 420-841 μm size range. Powder X-ray diffraction (XRD) indicated that only reflections assignable to quartz were present, matching International Centre for Diffraction Data powder diffraction file (PDF) #33-1161.

Nanoparticle Synthesis and Polymer Coating:

Size controlled synthesis¹⁶⁻²⁰ of MOF particles was performed by using chemical modulators that compete with metal binding sites, dramatically reducing the number of active sites for crystal growth.^{8,16,18,19} MIL-101(Cr) nanoparticles (NP) were prepared using a previously reported synthesis method^{21,22} in which terephthalic acid (139.6 mg, 0.82 mmol), modulator (4-methoxy benzoic acid; 5.1 mg, 0.033 mmol) and 25 mL of water were added to a fresh vial of $\text{Cr}(\text{NO}_3)_3 \cdot 9\text{H}_2\text{O}$ (330 mg, 0.82 mmol). The heterogeneous suspension was mixed thoroughly followed by sonication for five minutes at room temperature and then heated to 180 °C for 4 hours in a Teflon-lined autoclave. The reaction mixture was then cooled to room temperature and filtered with a 0.2 mm centrifuge filter to remove the unreacted/recrystallized terephthalic acid. After centrifuging the filtrate, the product was washed three times with water and methanol to obtain pure MIL-101(Cr) nanoparticles. As previously reported,^{21,22} as-synthesized MIL-101(Cr) nanofluid at an unadjusted pH of 5.5 was found to be colloiddally-stable and homogeneously dispersed for months, with high specific surface areas of 2917 m^2/g .

Stable polymer-coated nanoparticle suspensions were prepared by mixing polymer solutions with aqueous-dispersed nanoparticles in an Orbital Shaker for ~4 hours. Excess polymer in the solution was removed by highspeed centrifugation and the wet green pellet obtained was dispersed in water to obtain stable water dispersions of polymer coated MOF's for their use in nanoparticle transport study.

Nanoparticle Transport Experiments:

Transport of polymer-coated MIL-101(Cr) nanoparticles was evaluated by determining the quantity of MOF nanoparticles retained by the Accusand columns. Glass columns (10 cm diameter and 25 cm length) were used for studying nanoparticle transport and retention. Column was wet packed with Accusand and moisturized at a water content of about 10 % (*w/w*). To avoid blockage, we fitted the column with fritted discs (25-50 μm) to prevent any flux related issues. The estimated flow rate was 0.30 cm/min, resulting in a residence time of 10.5 min. The relatively high flow rates and resultant short residence times were chosen to minimize nanoparticle aggregation. Initially, uncoated nanoparticles were injected to understand the nanoparticle retention profile. Nanoparticle effluent from the column was collected, and the concentration of nanoparticles was measured via ultraviolet–visible (UV–Vis) spectrometry. UV-Vis spectrometry is a relatively inexpensive and commonly applied method for determining colloidal nanoparticle concentrations,²³ and MIL-101(Cr) is resistant to acidic dissolution techniques needed for elemental analysis. The absorbance of the samples was measured over a wavelength range of 300–800 nm and the results presented are the average of at least two measurements. The absorbance of <0.5 wt% colloidal MIL-101(Cr) water-based nanofluids are at ~560-580 nm.

Effect of Salinity on Transport Behavior of MOF Nanoparticles

Series of nanoparticle transport experiments were conducted to evaluate the transport behavior of MOF nanoparticles with and without polymer coating in saline environment. Transport experiments were conducted by wet packing the glass column with 50 g of Accusand with a pore volume of 14 mL. For estimating the effect of salinity on transport behavior of nanoparticles in Accusand, we used uncoated MOF nanoparticles and PSS-70K coated MOF nanoparticles. The packed column was first flushed with about 5 pore volumes (PV) of water or diluted NaCl (1M, 2 M or 5 M). Once the column is saturated with effluent, 3.7 pore volumes of MOF nanoparticle suspension (in water or in diluted NaCl (1M, 2 M or 5 M) was introduced into the column and allowed them to transport in the column. The column was further flushed with another 1 pore volume (14 mL) of effluent (water or diluted NaCl (1M, 2 M or 5 M). A total of 4.7 pore volumes of eluent is used in this transport study. The estimated flow rate was ~16 mL/min, resulting in a residence time of 4 min. Nanoparticle effluent from the column was collected, and the concentration of nanoparticles was measured via ultraviolet–visible (UV–Vis) spectrometry.

We used simple saturation method (porosity volume experiment) to estimate the pore volume of the Accusand. Known amount of Accusand was weighed and mixed with known volume of water. Glass column was wet packed, and the volume of the deionized water used at the saturation point in the column was noted. The pore volume of sand is determined by the difference between the total water volume before saturation and after.

Results And Discussions

We synthesized and characterized ~0.5 wt% nanofluids composed of polymer-coated MIL-101(Cr) nanoparticles, evaluating various polymers with different charges and functional groups (e.g. sulfonate, quaternary, and ammonium) as coatings to minimize nanoparticle agglomeration and retention in quartz (SiO₂)-hosted pore networks. Synthesis of MIL-101(Cr)-nanoparticles was accomplished using previously reported methods,^{21,22} and the polymers used for MIL-101(Cr) nanoparticle (NP) coatings included Poly(diallyldimethylammonium chloride) (PD), polyvinyl pyrrolidone (PVP), polyethylenimine (PEI), and Poly(sodium 4-styrenesulfonate) (PSS). PSS polymers with different average molecular weights of 70,000 and 200,000 were used to investigate size-dependent transport properties of polymer-coated NP, denoted as NP-PSS-70K and NP-PSS-200K.

Scanning electron microscopy imaging (SEM) characterization of our synthesized MOF nanoparticles revealed that the nearly spherical constituent nanoparticles were ~70 nm in diameter, and the overall morphological and size characteristics of the nanoparticles (NP-PD1, NP-PVP, NP-PEI and NP-PSS-70K) did not appear to change in response to polymer coatings (Figure 2). Water adsorption isotherms (**Figure S1**) revealed that the high sorption capacity (~150 wt%) of uncoated MIL-101(Cr) nanoparticles (NP) was minimally affected by polydadmac (PD1) coatings. However, other samples exhibited decreased water loading at 60% RH, including ~15% less uptake by NP-PSS-70K and ~60% less for both NP-PVP and NP-PEI. These results demonstrate that polymers may reduce access to MOF pore networks, and the polymers themselves may even partially occupy the pore volume. However, this polymer-coated MOF arrangement should not negatively impact their utility as acoustic contrast agents, as solvent-bearing (unactivated) MOFs still interact with acoustic waves,⁹ and the polymers may even increase low-frequency attenuation, similar to the behavior of long-chain hydrocarbons.²⁴

As expected, the addition of polymer coatings altered the hydrodynamic and electrokinetic properties of the nanoparticles. Dynamic light scattering (DLS) showed that the hydrodynamic diameter of NP at an unadjusted pH of 5.5 was 116 nm (**Table S1**), but hydrodynamic diameters increased up to 632 nm for NP-PSS-200K, for a general trend of NP<PEI≈PD≈PVP<PSS (Figure 3a). The addition of PD, PEI, and PVP polymer coatings also decreased the zeta potential of the nanofluids relative to the ~+35 mV NP nanofluid (**Table S1**, Figure 3a), making the polymer-coated nanoparticles more likely to aggregate. The zeta potentials of PSS-coated samples were around -27 mV, confirming that the particles have net negative charges, and the high absolute value indicates that the PSS-coated samples are as colloidally-stable as the uncoated MIL-101(Cr) in distilled water. Overall, the ability to engineer nanoparticles with varying surface charges is a key result, as this allows the nanofluid injectate to be tailored to the subsurface reservoir composition, including for lithologies with negative (sandstone), positive (carbonates), or highly heterogenous surface charges (mudstones or clay-rich sandstones).

The most novel aspect of this present investigation is the transport behavior of MOFs in environmentally-relevant porous media. To evaluate transport of MOF nanoparticles through porous media, we conducted flow-through column tests in which nanofluids passed through glass columns (10 cm diameter and 25

cm length) initially filled with water-saturated (10% w/w) quartz sand. Nanofluids had a linear flow rate of ~0.30 cm/min and a subsequent 10.5-minute residence time in the column. Accusand¹³ was used as a model geo-substrate for column packing due to its well defined quartz grain size distribution, consistent morphology, and relevant mineralogy for sandstone reservoirs,^{1,11} and common use in nanoparticle transport studies.^{14,15} Retention of nanoparticles was determined by measuring nanoparticle concentrations in the effluent via ultraviolet-visible spectrometry (UV-Vis) methods.

Above a pH of ~2.5, silica sand has a net negative surface charge,^{25,26} so it was expected that negatively-charged PSS-coated nanoparticles (**Table S1**) would most effectively be transported through the columns due to net electrostatic repulsion and subsequent unfavorable conditions for attachment. Indeed, only ~9% of NP-PSS-70K was retained in the core during the flow-through experiment (Figure 3b, **Table S1**). The large hydrodynamic diameter of NP-PSS-200K relative to all other nanoparticles (Figure 3a) was likely responsible for the >3X increase in retention relative to the NP-PSS-70K sample (Figure 3b), especially considering that the two PSS-based nanofluids have nearly identical zeta potentials (**Table S1**, Figure 3). Additionally, SEM imaging (Figure 2) suggested that the NP-PSS-200K particles were more agglomerated after transport through the column, a characteristic that would not promote efficient transport. The $\geq 25\%$ retention of the polymer-coated (PEI, PD, PVP) nanoparticles with positive surface potentials was consistent with the hypothesis that electrostatic attraction predominantly drives particle retention. Of the three, NP-PEI was the least effective nanofluid in terms of transportability, likely due to a combination of low zeta potential of +8 and its tertiary amine functional group, which has a strong affinity for negatively-charged surfaces (**Table S1**). SEM imaging of particles collected from the column effluent clarified that no observable changes in the size and/or morphology of individual nanoparticles were induced by transport through porous media (Figure 2).

Finally, although the uncoated MIL-101(Cr) nanofluid has a net positive charge (Figure 3a), only 11% of the particles were retained in the Accusand column. As we have previously injected this polymer-free nanofluid through a sandstone rock core,¹⁰ this result wasn't unexpected, although we didn't anticipate NP's mobility in siliceous porous media would be on par with that of NP-PSS-70K. We suggest that the small effective size of the uncoated NP partly contributes to its high mobility, as it has the smallest hydrodynamic diameter of 116 nm, less than half the size of NP-PSS-70K. Additionally, nanoscale surface charge heterogeneities in Accusand have been implicated for causing anomalous nanoparticle (de)sorption behavior.¹⁴ Namely, although it may be electrostatically-favorable for nanoparticles to adsorb to surface sites, thick electric double layers (EDL) at low ionic strength solution conditions may impede nanoparticle approach to attachment sites.¹⁴ This paradigm is consistent with our experimental setup, as the MOF nanoparticles are all dispersed in ultrapure water²⁷ to make nanofluids. Therefore, as the ionic strength increases, we would expect NP retention to increase dramatically relative to polymer-coated MOFs, like NP-PSS-70K, as the EDL becomes thinner.²⁸

Nanofluid stability under different solution conditions (e.g. pH and salinity) is an active area of research for us because the high salt concentrations can reduce the electrostatic repulsion leading to flocculation

behavior. We further investigated the effect of salinity on transport behavior of uncoated and polymer coated MOF nanoparticles in Accusand. Figure 4 illustrates the transport behavior of polymer coated nanoparticles with and without ionic strength solutions. The normalized effluent concentrations were plotted vs. the number of pore volumes passed through Accusand column. From Figure 4a and **Table S2** it is evident that there is significant retention (~29%) of nanoparticles observed when the transport of uncoated MIL-101(Cr) nanoparticles (NP) were conducted using 1M NaCl solutions. In contrary, only about 9% of retention was observed when uncoated MIL-101(Cr) nanoparticles were transported using water (Figure 4b). Interestingly, when negatively charged PSS-coated nanoparticles were transported in 1 M NaCl, only about 8.4% of nanoparticles were retained in the column. When the ionic strength of the medium was increased to 2 M NaCl, we observed only about 9% NP-PSS-70K retention in the core during the flow-through experiment. When the ionic strength of the medium was further increased to 5 M NaCl, we still observed only 13% of NP-PSS-70K retained. Transport experiments confirmed that polymer poly(sodium 4-styrenesulfonate; PSS), an adsorbing polymer not only enhances the colloidal stability of nMIL-101 (NP) at room temperature but also plays critical role in the transport of nanoparticles in porous siliceous media (Figure 4c). Although the presence of high concentration of ions at high salt concentrations can enhance the interactions of the ionic groups on polymers, the sodium salt of polystyrene sulfonate polymer on MOF nanoparticles provides electrostatic repulsion, as characterized by the zeta potential (ζ).^{29,30} These results reaffirm the role of nanoparticle surface characteristics on colloidal stability and their transport in environmentally relevant porous media.

Conclusion

In summary, we have demonstrated that the polymer coating on MOF nanoparticles will have significant impact on their transport in porous media. To the best of our knowledge, these results represent the first report on the transport properties of polymer-coated MOF-nanoparticles in environmentally relevant porous media. Of the polymer-coated nanoparticles studied, NP-PSS-70K was best able to migrate through the sand columns without being retained, and PEI-coated nanoparticles exhibited the worst performance, as over 50% of the particles did not pass through the Accusand. The PEI results especially emphasize that complex nanoparticle-fluid-rock interactions must be understood for successful utilization of nanofluid technologies in the subsurface. Surface adsorption of nanoparticles onto mineral interfaces must be minimized for successful injection and operation of novel seismic contrast agents, and retention is dominantly controlled by solution ionic strength, nanoparticle surface potentials, exposed functional groups, and effective size of colloids. To that end, we have designed, synthesized, and tested different polymer-coated MOF nanofluids with varying surface charges and functionalities that may be deployed in a variety of subsurface reservoirs with varying formation fluid chemistry and rock types.

Declarations

Acknowledgements:

This material is based on work supported by the U.S. Department of Energy Office of Fossil Energy (DOE FE) at PNNL through the National Energy Technology Laboratory, Morgantown, WV.

Author Contributions:

Satish K. Nune: Conceptualization, Writing - original draft, Formal analysis, Investigation, Methodology and Validation. Quin R.S. Miller: Formal analysis, Writing - review & editing, Visualization and Data Curation. H. Todd Schaef: Conceptualization, Formal analysis, Writing - review & editing, Data Curation, Project administration. Tengyue Jian: Formal analysis. Miao Song: Formal analysis. Dongsheng Li: Formal analysis. B. Peter McGrail: Conceptualization, Funding acquisition, Resources, Supervision, Writing - review & editing

Competing Interests:

The authors declare no competing interests.

References

1. Schaef, H. T. *et al.* Injectable contrast agents for enhanced subsurface mapping and monitoring., **114**, 3764–3770 (2017).
2. Elsaidi, S. K. *et al.* Extraction of rare earth elements using magnetite@MOF composites. *Journal of Materials Chemistry A*, **6**, 18438–18443 <https://doi.org/doi:10.1039/C8TA04750B> (2018).
3. McGrail, B. P. *et al.* Metal-organic heat carrier nanofluids. *Nano Energy*, **2**, 845–855 <https://doi.org/doi:10.1016/j.nanoen.2013.02.007> (2013).
4. ShamsiJazeyi, H., Miller, C. A., Wong, M. S., Tour, J. M. & Verduzco, R. Polymer-Coated Nanoparticles for Enhanced Oil Recovery. *J Appl Polym Sci* **131**, doi:ARTN 4057610.1002/app.40576 (2014)
5. Hochella, M. F. *et al.* Natural, incidental, and engineered nanomaterials and their impacts on the Earth system., **363**, eaau8299 <https://doi.org/doi:10.1126/science.aau8299> (2019).
6. Furukawa, H., Cordova, K. E., O'Keeffe, M. & Yaghi, O. M. The Chemistry and Applications of Metal-Organic Frameworks., **341**, 974– <https://doi.org/doi:10.1126/science.1230444> (2013).
7. Yap, M. H., Fow, K. L. & Chen, G. Z. Synthesis and applications of MOF-derived porous nanostructures. *Green Energy Environ*, **2**, 218–245 <https://doi.org/doi:10.1016/j.gee.2017.05.003> (2017).
8. Marshall, C. R., Staudhammer, S. A. & Brozek, C. K. Size control over metal-organic framework porous nanocrystals. *Chem Sci*, **10**, 9396–9408 <https://doi.org/doi:10.1039/c9sc03802g> (2019).
9. Miller, Q. R. S. *et al.* Microporous and flexible framework acoustic metamaterials for sound attenuation and contrast agent applications. *ACS Appl. Mater. Interfaces*, **10**, 44226–44230 <https://doi.org/doi:10.1021/acsami.8b19249> (2018).

10. Férey, G. *et al.* A chromium terephthalate-based solid with unusually large pore volumes and surface area., **309**, 2040–2042 <https://doi.org/doi:10.1126/science.1116275> (2005).
11. Miller, Q. R. S. *et al.* Geophysical Monitoring with Seismic Metamaterial Contrast Agents. *Unconventional Resources Technology Conference (URTeC) Proceedings* **1123**, doi:<https://doi.org/10.15530/urtec-2019-1123> (2019)
12. Nune, S. K., Liu, J., Sinnwell, M. & McGrail, B. P. P.K., T. & Polymer-Functionalized Magnetic Particle Embodiments for Solute Separation and Devices and Systems for Using the Same. *US Patent (Filed)* (2020)
13. Schroth, M. H., Istok, J. D., Ahearn, S. J. & Selker, J. S. Characterization of Miller-similar silica sands for laboratory hydrologic studies. *SSSAJ*, **60**, 1331–1339 (1996).
14. Torkzaban, S., Kim, Y., Mulvihill, M., Wan, J. M. & Tokunaga, T. K. Transport and deposition of functionalized CdTe nanoparticles in saturated porous media. *J Contam Hydrol*, **118**, 208–217 <https://doi.org/doi:10.1016/j.jconhyd.2010.10.002> (2010).
15. Torkzaban, S., Wan, J. M., Tokunaga, T. K. & Bradford, S. A. Impacts of bridging complexation on the transport of surface-modified nanoparticles in saturated sand. *J Contam Hydrol*, **136**, 86–95 <https://doi.org/doi:10.1016/j.jconhyd.2012.05.004> (2012).
16. Morris, W. *et al.* Role of Modulators in Controlling the Colloidal Stability and Polydispersity of the UiO-66 Metal-Organic Framework. *Acs Appl Mater Inter*, **9**, 33413–33418 <https://doi.org/doi:10.1021/acsami.7b01040> (2017).
17. Zhao, T. *et al.* Facile synthesis of nano-sized MIL-101(Cr) with the addition of acetic acid. *Inorg Chim Acta*, **471**, 440–445 <https://doi.org/doi:10.1016/j.ica.2017.11.030> (2018).
18. Jiang, D. M., Burrows, A. D. & Edler, K. J. Size-controlled synthesis of MIL-101(Cr) nanoparticles with enhanced selectivity for CO₂ over N₂., **13**, 6916–6919 <https://doi.org/doi:10.1039/c1ce06274c> (2011).
19. Zhao, T., Li, S. H., Shen, L., Wang, Y. & Yang, X. Y. The sized controlled synthesis of MIL-101(Cr) with enhanced CO₂ adsorption property. *Inorg Chem Commun*, **96**, 47–51 <https://doi.org/doi:10.1016/j.inoche.2018.07.036> (2018).
20. Carmona, F. J. *et al.* Coordination Modulation Method To Prepare New Metal-Organic Framework-Based CO-Releasing Materials. *Acs Appl Mater Inter*, **10**, 31158–31167 <https://doi.org/doi:10.1021/acsami.8b11758> (2018).
21. Annapureddy, H. V. R., Nune, S. K., Motkuri, R. K., McGrail, B. P. & Dang, L. E. X. A Combined Experimental and Computational Study on the Stability of Nanofluids Containing Metal Organic Frameworks. *J. Phys. Chem. B*, **119**, 8992–8999 <https://doi.org/doi:10.1021/jp5079086> (2015).
22. Nandasiri, M. I. *et al.* Increased Thermal Conductivity in Metal-Organic Heat Carrier Nanofluids. *Sci Rep-Uk* **6**, doi:ARTN 2780510.1038/srep27805(2016)
23. Hendel, T. *et al.* In Situ Determination of Colloidal Gold Concentrations with UV–Vis Spectroscopy: Limitations and Perspectives. *Anal. Chem*, **86**, 11115–11124 <https://doi.org/doi:10.1021/ac502053s> (2014).

24. Behura, J., Batzle, M., Hofmann, R. & Dorgan, J. Heavy oils: Their shear story. *Geop*, **72**, E175–E183 (2007).
25. Jada, A., Ait Akbour, R. & Douch, J. Surface charge and adsorption from water onto quartz sand of humic acid., **64**, 1287–1295 <https://doi.org/doi:10.1016/j.chemosphere.2005.12.063> (2006).
26. Kosmulski, M., Eriksson, P., Gustafsson, J. & Rosenholm, J. B. Specific adsorption of nickel and ζ potential of silica at various solid-to-liquid ratios. *J. Colloid Interface Sci*, **220**, 128–132 (1999).
27. De, S. *et al.* Water-Based Assembly of Polymer-Metal Organic Framework (MOF) Functional Coatings. *Adv Mater Interfaces* **4**, doi:ARTN 160090510.1002/admi.201600905(2017)
28. Moore, D. M. & Reynolds, R. C. *X-Ray Diffraction and the Identification and Analysis of Clay Minerals* (Oxford University Press, 1989).
29. Bagaria, H. G. *et al.* Stabilization of Iron Oxide Nanoparticles in High Sodium and Calcium Brine at High Temperatures with Adsorbed Sulfonated Copolymers., **29**, 3195–3206 (2013).
30. Yuan, H. Y. & Liu, G. M. Ionic effects on synthetic polymers: from solutions to brushes and gels., **16**, 4087–4104 (2020).

Figures

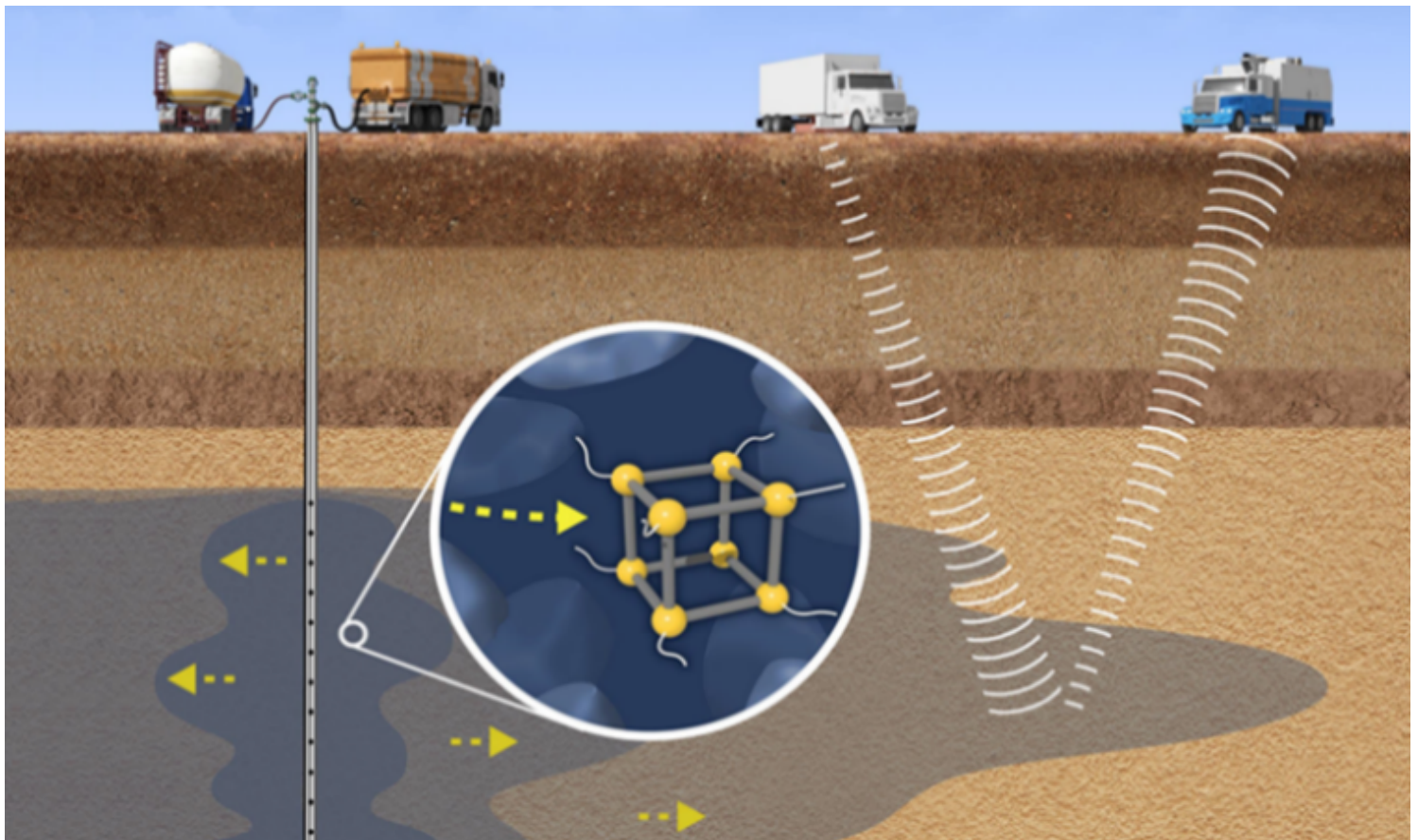


Figure 1

Illustration of low-frequency absorptive metal-organic frameworks acoustic nanomaterials injected into the subsurface to track fluids and map complex structures

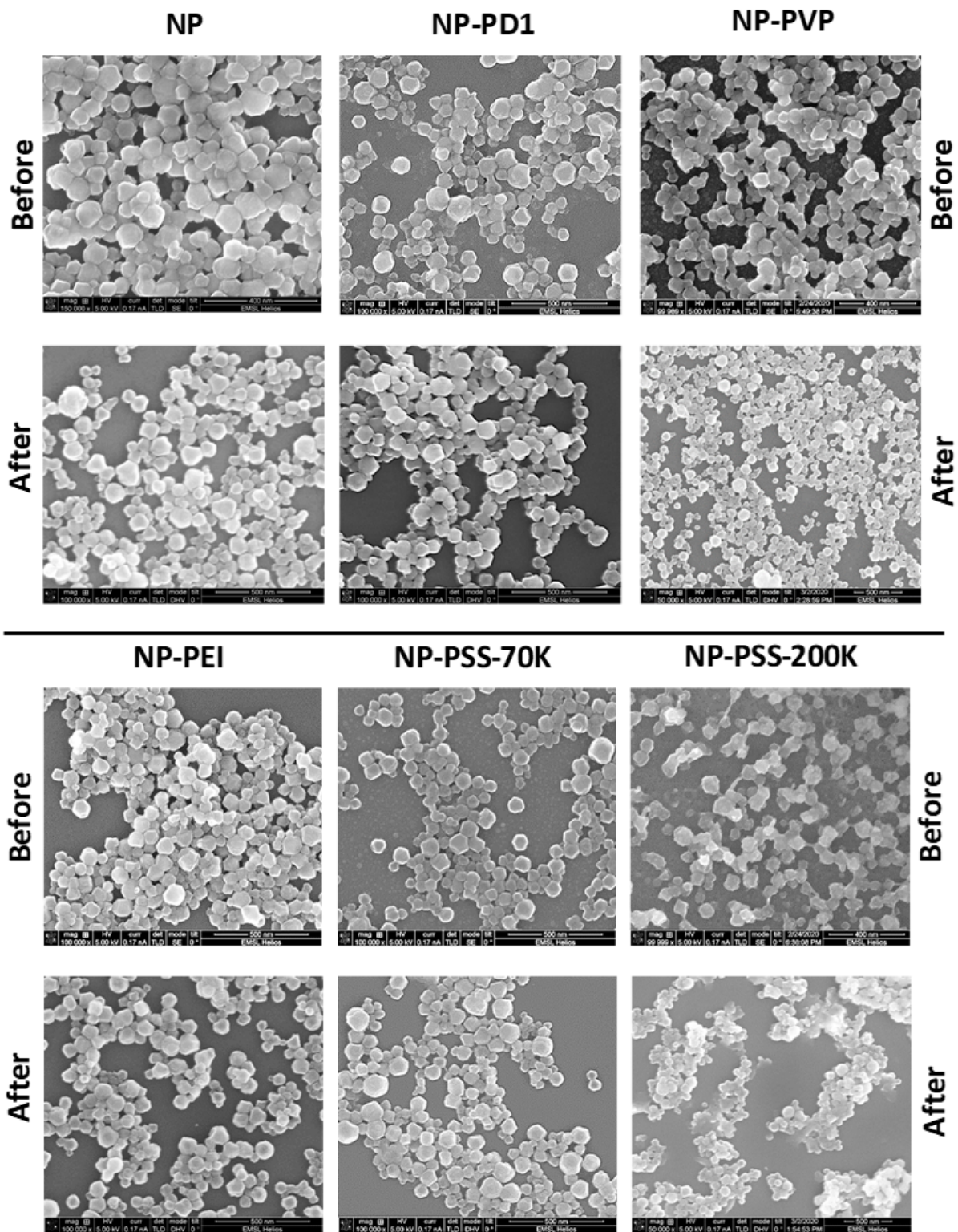


Figure 2

SEM images of MOF nanoparticles with different polymer coatings before and after Accusand column transport experiments. Scale bars are all 500 nm, except for the “before” panels for NP, NP-PVP, and NP-PSS-200K, as those have 400 nm scale bars.

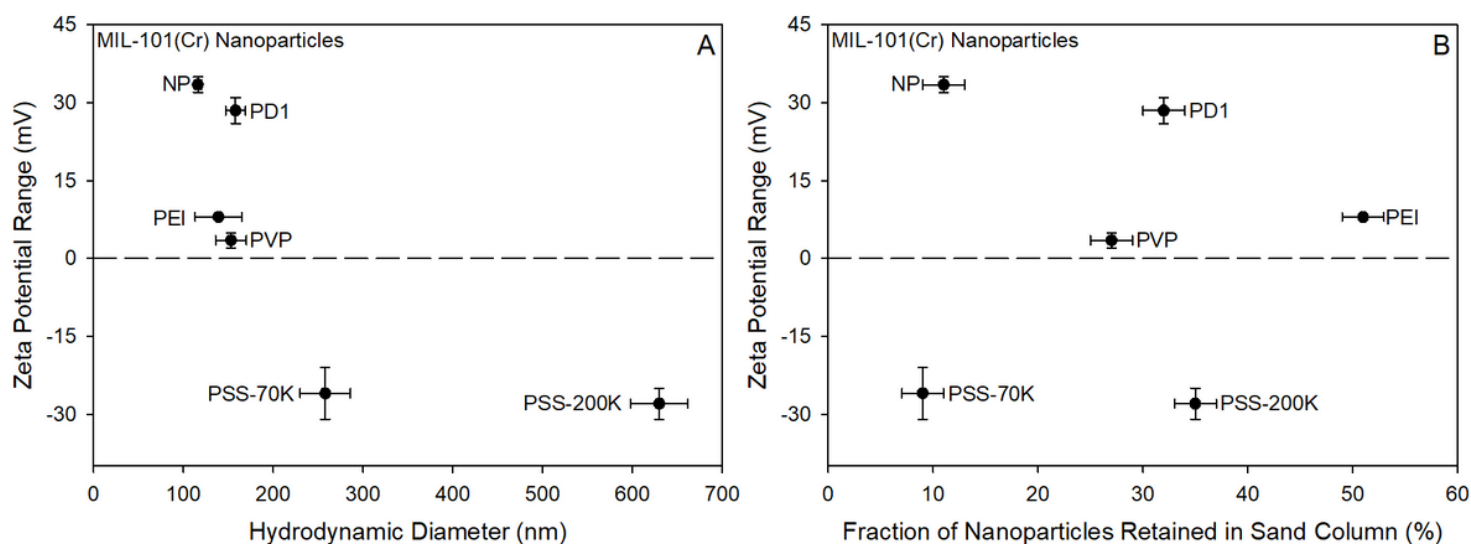


Figure 3

(A) Zeta potential ranges and hydrodynamic radii of synthesized MIL-101(Cr) MOF nanoparticles and polymer-coated MOF nanoparticles at unadjusted pH of 5.5. (B) Results of flow-through transport experiments, showing how nanoparticle retention by Accusand was influenced by the polymer coating and electrokinetic

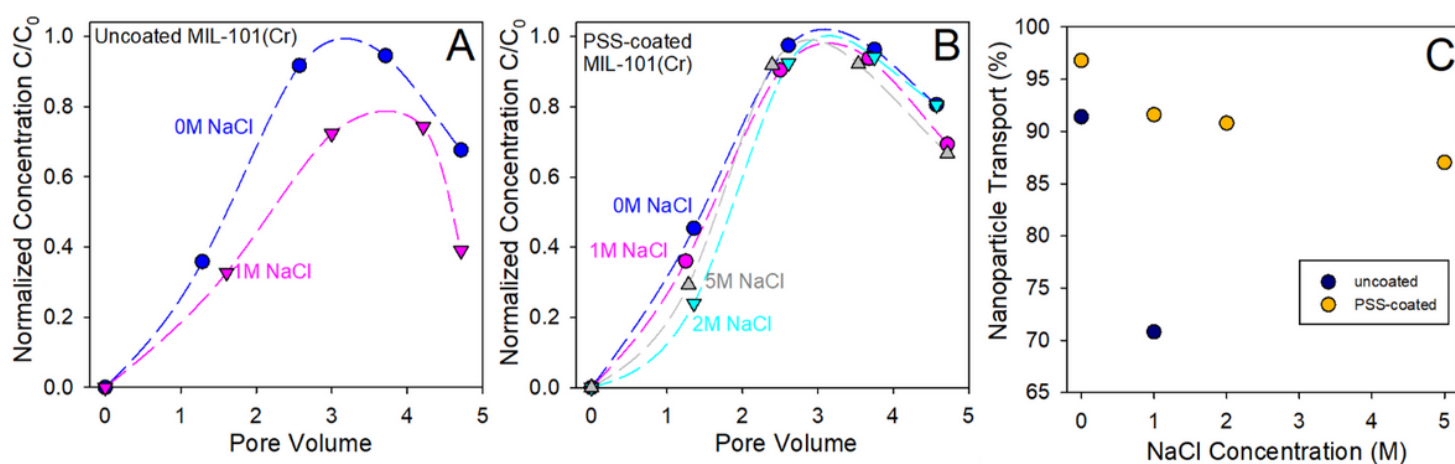


Figure 4

(A) Transport of uncoated nanoparticles (NP) in water and 1M NaCl, (B) Transport of polymer-coated MOF nanoparticles (NP-PSS-70K) in water, 1, 2, and 5M NaCl, (C) Comparison of nanoparticle transport for different salinity and particle type.

Supplementary Files

This is a list of supplementary files associated with this preprint. Click to download.

- [SupportingInformation.docx](#)